

1 **Soil erosion by snow gliding – a first quantification attempt in a sub-**  
2 **alpine area, Switzerland**

3

4 K. Meusburger<sup>1</sup>, G. Leitinger<sup>2</sup>, L. Mabit<sup>3</sup>, M. H. Mueller<sup>1</sup>, A. Walter<sup>1</sup> and C.  
5 Alewell<sup>1</sup>

6

7 <sup>1</sup> Environmental Geosciences, University of Basel, Basel, Switzerland

8 <sup>2</sup> Institute of Ecology, University of Innsbruck, Innsbruck, Austria

9 <sup>3</sup> Soil and Water Management & Crop Nutrition Laboratory, Joint FAO/IAEA  
10 Division of Nuclear Techniques in Food and Agriculture, International Atomic  
11 Energy Agency, Austria

12

13 **Abstract**

14 Snow processes might be one important driver of soil erosion in Alpine grasslands  
15 and thus the unknown variable when erosion modelling is attempted. The aim of  
16 this study is to assess the importance of snow gliding as soil erosion agent for  
17 four different land use/land cover types in a sub-alpine area in Switzerland. We  
18 used three different approaches to estimate soil erosion rates: sediment yield  
19 measurements in snow glide depositions, the fallout radionuclide <sup>137</sup>Cs, and  
20 modelling with the Revised Universal Soil Loss Equation (RUSLE). RUSLE permits the  
21 evaluation of soil loss by water erosion, the <sup>137</sup>Cs method integrates soil loss due  
22 to all erosion agents involved, and the snow glide deposition sediment yield  
23 measurement can be directly related to snow glide induced erosion. Further,  
24 cumulative snow glide distance was measured for the sites in the winter  
25 2009/2010 and modelled for the surrounding area and long-term average winter

26 precipitation (1959-2010) with the Spatial Snow Glide Model (SSGM). Measured  
27 snow glide distance confirmed the presence of snow gliding and ranged from 2  
28 to 189 cm, with lower values at the north facing slopes. We observed a  
29 reduction of snow glide distance with increasing surface roughness of the  
30 vegetation, which is important information with respect to conservation  
31 planning and expected and ongoing land use changes in the Alps. Snow glide  
32 erosion estimated from the snow glide depositions was highly variable with  
33 values ranging from 0.03 to 22.9 t ha<sup>-1</sup> yr<sup>-1</sup> in the winter 2012/2013. For sites  
34 affected by snow glide deposition, a mean erosion rate of 8.4 t ha<sup>-1</sup> yr<sup>-1</sup> was  
35 found. The difference in long-term erosion rates determined with RUSLE and <sup>137</sup>Cs  
36 confirm the constant influence of snow glide induced erosion, since a large  
37 difference (lower proportion of water erosion compared to total net erosion)  
38 was observed for sites with high snow glide rates and vice versa. Moreover, the  
39 difference of RUSLE and <sup>137</sup>Cs erosion rates was related to the measured snow  
40 glide distance ( $R^2 = 0.64$ ;  $p < 0.005$ ) and to the snow deposition sediment yields  
41 ( $R^2 = 0.39$ ;  $p = 0.13$ ). The SSGM reproduced the relative difference of the  
42 measured snow glide values under different land uses and land cover types. The  
43 resulting map highlighted the relevance of snow gliding for large parts of the  
44 investigated area. Based on these results, we conclude that snow gliding  
45 appears to be a crucial and non-negligible process impacting soil erosion  
46 pattern and magnitude in sub-alpine areas with similar topographic and  
47 climatic conditions.

48

49 Keywords: soil erosion, Alps, snow, <sup>137</sup>Cs, RUSLE

50

## 51 1 Introduction

52 While rainfall is a well-known agent of soil erosion, the erosive forces of snow  
53 movements are qualitatively recognized but quantification has not been  
54 achieved yet (Leitinger et al., 2008; Konz et al., 2012). Particularly wet  
55 avalanches can yield enormous erosive forces that are responsible for major soil  
56 loss (Gardner, 1983; Ackroyd, 1987; Bell et al., 1990; Jomelli and Bertran, 2001;  
57 Heckmann et al., 2005; Fuchs and Keiler, 2008; Freppaz et al., 2010) also in the  
58 avalanche release area (Ceaglio et al., 2012).

59 Besides avalanches another important process of snow movement affecting the  
60 soil surface is snow gliding (In der Gand and Zupancic, 1966). Snow gliding is the  
61 slow (mm to cm per day) downhill motion of a snowpack over the ground  
62 surface caused by the stress of its own weight (Parker, 2002). Snow gliding  
63 predominantly occurs on south-east to south-west facing slopes with slope  
64 angles between 30-40° (In der Gand and Zupancic, 1966; Leitinger et al., 2008).  
65 Two main factors that control snow glide rates are (i) the wetness of the  
66 boundary layer between the snow and soil cover and (ii) the ground surface  
67 roughness determined by the vegetation cover and rocks (McClung and Clarke,  
68 1987; Newesely et al., 2000). So far, only few studies investigated the effect of  
69 snow gliding on soil erosion (Newesely et al., 2000; Leitinger et al., 2008). A  
70 major reason for this shortcoming is the difficulty to obtain soil erosion rates  
71 caused by snow processes. In steep sub-alpine areas soil erosion records (e.g.  
72 with sediment traps) are restricted to the vegetation period because  
73 avalanches and snow gliding can irreversibly damage the experimental design  
74 (Konz et al., 2012).

75 Recently, first physically based attempts to model the erosive force of wet  
76 avalanches were done (Confortola et al., 2012). No similar model exists for snow

77 gliding. However, the potential maximum snow glide distance during a targeted  
78 period can be modelled with the empirical Spatial Snow Glide Model (SSGM)  
79 (Leitinger et al., 2008). The modelling of this process is crucial to evaluate the  
80 impact of the snow glide process on soil erosion at larger scale.

81 Soil erosion rates can be obtained by direct quantification of sediment transport  
82 in the field, by fallout radionuclides (FRN) based methods (e.g. Mabit et al.,  
83 1999; Benmansour et al., 2013; Meusburger et al., 2013) and by soil erosion  
84 models (Nearing et al., 1989; Merritt et al., 2003). Since the end of the 1970's  
85 empirical soil erosion models such as the Universal Soil Loss Equation (USLE;  
86 Wischmeier and Smith, 1965; Wischmeier and Smith, 1978), and its refined  
87 versions the Revised USLE (RUSLE; Renard et al., 1997) and the Modified USLE  
88 (MUSLE; Smith et al., 1984), have been used worldwide to evaluate soil erosion  
89 magnitude under various conditions (Kinnell, 2010). These well-known models  
90 allow the assessment of sheet erosion and rill/inter-rill erosion under moderate  
91 topography. However, they do not integrate erosion processes associated with  
92 wind, mass movement, tillage, channel or gully erosion (Risse et al., 1993; Mabit  
93 et al., 2002; Kinnell, 2005) and also snow impact due to movement is not  
94 considered (Konz et al., 2009). Several models have been tested for steep alpine  
95 sites with the result that RUSLE reproduced the magnitude of soil erosion, the  
96 relative pattern and the effect of the vegetation cover most plausible (Konz et  
97 al., 2010; Meusburger et al., 2010b; Panagos et al., 2014). The erosion rate  
98 derived from RUSLE corresponds to water erosion induced by rainfall and surface  
99 runoff and hence in our site to the soil erosion processes during the summer  
100 season without significant influence of snow processes.

101 In contrast, the translocation of FRN reflects all erosion processes by water, wind  
102 and snow during summer and winter season and thus, is an integrated estimate  
103 of the total net soil redistribution rate since the time of the fallout in the 1950s

104 (the start of the global fallout deposit) and in case of predominant Chernobyl  
105  $^{137}\text{Cs}$  input since 1986. Anthropogenic fallout radionuclides have been used  
106 worldwide since decades to assess the magnitude of soil erosion and  
107 sedimentation processes (Mabit and Bernard, 2007; Mabit et al., 2008; Matisoff  
108 and Whiting, 2011). The most well-known conservative and validated  
109 anthropogenic radioisotope used to investigate soil redistribution and  
110 degradation is  $^{137}\text{Cs}$  (Mabit et al., 2013).

111 For (sub-) alpine areas the different soil erosion processes captured by RUSLE  
112 and the  $^{137}\text{Cs}$  method result in different erosion rates (Konz et al., 2009; Juretzko,  
113 2010; Alewell et al., 2014; Stanchi et al., 2014, accepted). However, this  
114 difference might also be due to several other reasons such as the error of both  
115 approaches, the non-suitability of the RUSLE model for this specific environment  
116 and/or the erroneous estimation of the initial fallout of  $^{137}\text{Cs}$ .

117 In this study, we aim to quantify snow glide induced erosion and investigate,  
118 whether the observed discrepancy between erosion rates estimated with RUSLE  
119 and the ones provided by the  $^{137}\text{Cs}$  method can be at least partly attributed to  
120 snow gliding processes. Since vegetation cover affects snow gliding, four  
121 different sub-alpine land use/land cover types were investigated. A further  
122 objective of our research is to assess the relevance of snow gliding processes at  
123 catchment scale using the Spatial Snow Glide Model (SSGM).

## 124 **2 Materials and Methods**

### 125 *2.1 Site description*

126 The study site is located in Central Switzerland (Canton Uri) in the Ursern Valley  
127 (Fig. 1). The elevation of the W-E extended alpine valley ranges from 1400 up to  
128 2500 m a.s.l. At the valley bottom (1442 m a.s.l.), average annual air  
129 temperature for the years 1980–2012 is around  $4.1 \pm 0.7$  °C and the mean annual  
5

130 precipitation is  $1457 \pm 290$  mm, with 30% falling as snow (MeteoSwiss, 2013). The  
131 valley is snow covered from November to April with a mean annual snow height  
132 of 67cm in the period 1980 to 2012. Drainage of the basin is usually controlled by  
133 snowmelt from May to June. Important contribution to the flow regime takes  
134 place during early autumn floods. The land use is characterised by hayfields  
135 near the valley bottom (from 1450 to approximately 1650 m a.s.l.) and pasturing  
136 further upslope. Siliceous slope debris and moraine material is dominant at our  
137 sites, and forms Cambisols (Anthric) and Podzols (Anthric) classified after IUSS  
138 Working Group (2006).

139 Of the 14 experimental sites, 9 are located at the south-facing slope and 5 at  
140 the north-facing slope at altitudes between 1476 and 1670 m a.s.l. Four different  
141 land use/cover types with 3-5 replicates each were investigated: hayfields (h),  
142 pastures (p), pastures with dwarf shrubs (pw), and abandoned grassland  
143 covered with *Alnus viridis* (A). Vegetation of hayfields is dominated by *Trifolium*  
144 *pratense*, *Festuca* sp., *Thymus serpyllum* and *Agrostis capillaris*. For the pastured  
145 grassland *Globularia cordifolia*, *Festuca* sp. and *Thymus serpyllum* dominate.  
146 Pastures with dwarf shrubs are dominated by *Calluna vullgaris*, *Vaccinium*  
147 *myrtillus*, *Festuca violacea*, *Agrostis capillaris* and *Thymus serpyllum*. At pasture  
148 sites of the south facing slope, which are stocked from June to September,  
149 cattle trails transverse to the main slope direction.

## 150 2.2 Snow glide measurement

151 We measured cumulative snow glide distances with snow glide shoes for the  
152 winter 2009/2010. The snow glide shoe equipment was similar to the set-up used  
153 by In der Gand and Zupancic (1966), Newesely et al. (2000) and Leitinger et al.  
154 (2008). The set-up consisted of a glide shoe and a buried weather-proof box  
155 with a wire drum. Displacement of the glide shoe causes the drum to unroll the

156 wire. The total unrolled distance was measured in spring after snowmelt. To  
157 prevent entanglement with the vegetation, the steel wire was protected by a  
158 flexible plastic tube. For each site, 3 to 5 snow glide shoes were installed to  
159 obtain representative values. A total of 60 devices were used.

### 160 2.3 Assessment of soil redistribution

161 Snow glide distance was measured with snow glide shoes for 14 sites. For 12 of  
162 the 14 sites (exclusive of the two *Alnus viridis* sites at the north facing slopes  
163 (AN)), RUSLE and <sup>137</sup>Cs based erosion rates were assessed. Seven of these sites  
164 were measured in 2007 (Konz et al., 2009). During a second field campaign  
165 performed in 2010, 5 additional sites were investigated using the same methods  
166 for soil erosion assessment with <sup>137</sup>Cs and RUSLE as in 2007 (Konz et al., 2009). The  
167 <sup>137</sup>Cs measurements were decay corrected to 2007 for comparison purpose.

#### 168 2.3.1 Snow and sediment sampling in the snow glide deposition area

169 Sediment concentrations were estimated by measuring the amount of sediment  
170 in snow samples taken with a corer from the snow glide depositions in spring  
171 2013 (Fig. 2). The corer allowed for the sampling of the entire depth of the snow  
172 deposition and thus the integration of the sediment yield over the depth of the  
173 deposition. For larger depositions, samples were collected along two transects  
174 across each deposition. For smaller depositions, we took three samples. The  
175 samples were melted and filtered through a 0.11 µm filter. The filtered material  
176 was dried at 40°C and weighted to obtain the concentration of sediment per  
177 sample ( $M_s$ ). The mean sediment values (and for depositions with several  
178 samples the interpolated mean sediment values) were used to estimate the total  
179 sediment load of the snow-glide deposition ( $M_A$ ) according to:

$$180 \quad M_A = \frac{A_A \times M_s}{A_c} \quad \text{Equation 1}$$

181 where  $A_c$  is the area of the corer and  $A_A$  is the area of the snow-glide  
182 deposition. The latter was mapped in the field by GPS and measuring tape.  
183 Sediment load was further converted to soil erosion rate (E) by:

$$184 \quad E = \frac{MA}{A_S} \quad \text{Equation 2}$$

185 where  $A_s$  is the source area of the snow and sediment deposition. Each snow  
186 glide was photo documented and the respective source area was mapped with  
187 GPS and transferred to ArcGIS for surface area estimation.

### 188 2.3.2 Assessment of soil redistribution by water erosion using the RUSLE

189 The USLE (Wischmeier and Smith, 1978) and its revised version the RUSLE (Renard  
190 et al., 1997) is an empirical erosion model originally developed in the United  
191 States. Several adapted versions for other regions as well as for different  
192 temporal resolutions have been developed and applied with more or less  
193 success (Kinnell, 2010). Despite its well-known limitation (highlighted in our  
194 introduction), we selected RUSLE because of the lack of simple soil erosion  
195 models specific for mountain areas and moreover because of its better  
196 performance when compared to the other existing models (Konz et al., 2010;  
197 Meusburger et al., 2010b). The RUSLE can be calculated using the following  
198 equation:

$$199 \quad A = R \times K \times LS \times C \times P \quad \text{Equation 3}$$

200  
201  
202 where  $A$  is the predicted average annual soil loss ( $t \text{ ha}^{-1} \text{ yr}^{-1}$ ).  $R$  is the rainfall-  
203 runoff-erosivity factor ( $N \text{ h}^{-1}$ ) that quantifies the effect of raindrop impact and  
204 reflects the rate of runoff likely to be associated with the rain (Renard et al.,  
205 1997). The soil erodibility factor  $K$  ( $N \text{ h kg m}^{-2}$ ) reflects the ease of soil



206 detachment by splash or surface flow. The parameter  $LS$  (dimensionless)  
207 accounts for the effect of slope length ( $L$ ) and slope gradient ( $S$ ) on soil loss. The  
208 C-factor is the cover factor, which represents the effects of all interrelated  
209 cover and management variables (Renard et al., 1997).

210 For comparability between the RUSLE estimates of Konz et al. (2009) and the  
211 ones assessed in this study we used the same R-factor approximation of Rogler  
212 and Schwertmann (1981) adapted by Schuepp (1975). According to the USLE  
213 procedure, snowmelt can be integrated in erosivity calculation by multiplying  
214 snow precipitation by 1.5 and then adding the product to the kinetic energy  
215 times the maximum 30-min intensity. However, the latter procedure does not  
216 account for redistribution of snow by drifting, sublimation, and reduced  
217 sediment concentrations in snowmelt (Renard et al., 1997). Therefore, as  
218 suggested by Renard (1997) this adaption of the R-factor was not considered in  
219 this study. The K-factor was calculated with the K nomograph after Wischmeier  
220 and Smith (1978) using grain-size analyses and carbon contents of the upper 15  
221 cm of the soil profiles. Total C content of soils was measured with a Leco CHN  
222 analyzer 1000, and grain size-analyses were performed with sieves for grain sizes  
223 between 32 and 1000  $\mu\text{m}$  and with a Sedigraph 5100 (Micromeritics) for grain  
224 sizes between 1 and 32  $\mu\text{m}$ .  $L$  and  $S$  were calculated after Renard et al. (1997).  
225 The support and practice factor  $P$  (dimensionless) was set to 0.9 for some of the  
226 pasture sites because alpine pastures with cattle trails resemble small terrace  
227 structures, which are suggested to be considered in  $P$  (Foster and Highfill, 1983).  
228 For all other sites,  $P$  value was set to 1. The cover-and-management factor  $C$   
229 was assessed for sites with and without dwarf shrubs separately using measured  
230 fractional vegetation cover (FVC) in the field.

231 For investigated sites without dwarf shrubs (US Department of Agriculture,  
232 1977) the C-factor can be estimated with:

233

234  $C = 0.45 \times e^{-0.0456 \times FVC}$  Equation 4

235

236 and for sites with dwarf shrubs the following equation was used:

237

238  $C = 0.45 \times e^{-0.0324 \times FVC}$  Equation 5

239

240 The *FVC* was determined in April and September using a grid of 1 m<sup>2</sup> with a mesh  
241 width of 0.1 m<sup>2</sup>. The visual estimate of each mesh was averaged for the entire  
242 square meter. This procedure was repeated four times for each plot. The  
243 maximum standard deviation was approx. 5%. For the *Alnus viridis* sites we used  
244 the value provided by the US Department of Agriculture (1977) i.e. 0.003. This  
245 value assumes a fall height of 0.5 m and a ground cover of 95-100%.

246 The uncertainty assessment of the RUSLE estimates is based on the measurement  
247 error of the plot steepness ( $\pm 2\%$ ), which was determined by repeated  
248 measurements and slope length ( $\pm 12.5$  m). An error of  $\pm 2\%$  was assumed for the  
249 grain size analyses as well as for the organic carbon determination. These errors  
250 were propagated through the *K*-factor calculation. An error of  $\pm 20\%$  based on  
251 the observed variability between spring and autumn of *FVC* on the plots, was  
252 used for the determination of the *C*-factor. For the *R*-factor an error of  $\pm 5$  N h<sup>-1</sup>,  
253 which corresponds to the observed variability between the sites was assumed.  
254 Finally error propagation for the multiplication of the single RUSLE factors was  
255 done.

### 256 2.3.3 <sup>137</sup>Cs to assess total net soil redistribution

257 A 2 x 2 inch NaI-scintillation detector (Sarad, Dresden, Germany) was used to  
258 measure the in-situ <sup>137</sup>Cs activity. The detector was mounted perpendicular to

259 the ground at a height of 25 cm to reduce the radius of the investigated area to  
260 1 meter. Measurement time was set at 3600 seconds and each site was  
261 measured three times.

262 The detector was successfully ( $R^2 = 0.86$ ) calibrated against gamma  
263 spectroscopy laboratory measurements with a 20% relative efficiency Li-drifted  
264 Ge detector (GeLi; Princeton Gamma-Tech, Princeton, NJ, USA) at the  
265 Department for Physics and Astronomy, University of Basel. For the GeLi detector  
266 the resulting measurement uncertainty on  $^{137}\text{Cs}$  peak area (at 662 keV) was  
267 lower than 8% (error of the measurement at 1-sigma) (Schaub et al.,  
268 2010). Gamma spectrometry calibration and quality control of the analysis were  
269 performed following the protocol proposed by Shakhshiro and Mabit (2009).

270 Soil moisture influences the measured  $^{137}\text{Cs}$  activity. Thus, soil moisture  
271 measurements with an EC-5 sensor (DecagonDevices) were used to correct the  
272 in-situ measurements. The NaI detector has the advantage of providing an  
273 integrated measurement over an area of 1 m<sup>2</sup>. The commonly observed intrinsic  
274 small scale variability (~30 %) for  $^{137}\text{Cs}$  (Sutherland, 1996; Kirchner, 2013) is thus,  
275 smoothed. Nonetheless, around 10% of the uncertainty of the  $^{137}\text{Cs}$ -based soil  
276 erosion values can be attributed to the variability of replicated measurements  
277 on each single plot. The main error of the in-situ measurement results from the  
278 peak area evaluation and was determined at 17 % (Schaub et al., 2010).

279 With the  $^{137}\text{Cs}$  method soil redistribution rates are calculated by comparing the  
280 isotope inventory for an eroding point with a local reference inventory where  
281 neither erosion nor soil accumulation is expected. In the Urseren Valley, the  
282 initial reference  $^{137}\text{Cs}$  fallout originated from thermonuclear weapon tests in the  
283 1950s-1960s and the nuclear power plant accident of Chernobyl in 1986.

284 For the conversion of the  $^{137}\text{Cs}$  inventories to soil erosion rates knowledge about  
285 the proportion of Chernobyl  $^{137}\text{Cs}$  fallout is a key parameter for the estimation of  
11

286 erosion rates, however, only little data is available. Pre-Chernobyl (1986)  $^{137}\text{Cs}$   
287 activities of the top soil layers (0 – 5 cm) between 2 and 58  $\text{Bq kg}^{-1}$  (one outlier  
288 of 188  $\text{Bq kg}^{-1}$  in Ticino) were recorded for 12 sites distributed over Switzerland  
289 (Riesen et al., 1999). After radioactive decay, in 2007 only 1 – 35  $\text{Bq kg}^{-1}$  are left.  
290 The  $^{137}\text{Cs}$  activity for the flat reference sites near the valley bottom (1469-1616 m  
291 a.s.l) was estimated as  $146 \pm 20 \text{ Bq kg}^{-1}$  (Schaub et al., 2010). The investigated  
292 sites are located in close vicinity to the reference sites and at comparable  
293 altitude (1476-1670 m a.s.l). Consequently, the maximum contribution of pre-  
294 Chernobyl  $^{137}\text{Cs}$  might represent 20% at reference sites.

295 Additionally, vertical migration must be considered. In literature migration  
296 values between 0.03 and 1.30  $\text{cm yr}^{-1}$  are reported (Schimmack et al., 1989;  
297 Arapis and Karandinos, 2004; Schuller et al., 2004; Schimmack and Schultz, 2006;  
298 Ajayi et al., 2007). In the Urseren Valley,  $^{137}\text{Cs}$  activity ( $\text{Bq kg}^{-1}$ ) declines  
299 exponentially with soil depth. Therefore, for the conversion of  $^{137}\text{Cs}$   
300 measurements to soil erosion rates, the well-known profile distribution model  
301 (Walling et al., 2011) was adapted for the direct use with  $^{137}\text{Cs}$  activity profile  
302 (Konz et al., 2009; Konz et al., 2012). We set the particle size factor to 1,  
303 because no preferential transport of the finer soil particles was observed for our  
304 sites (Konz et al., 2012). In contrast, no preferential transport or preferential  
305 transport of coarse material occurred, most likely due to snow and animal  
306 induced particle transport (see Konz et al., 2012). The calculation of the erosion  
307 rates refers to the period 1986-2007 because pre-Chernobyl  $^{137}\text{Cs}$  is negligible.  
308 For uncultivated sites the Diffusion and Migration model is an alternative to the  
309 profile distribution model. However, the  $^{137}\text{Cs}$  depth profile at our reference sites  
310 did not follow a polynomial distribution and thus did not allow for a successful fit  
311 of the diffusion and migration coefficient. Due to the integrative and repeated  
312 measurement with the NaI detector, the errors associated with measurement

12

313 precision are assumed to be largely cancelled out. However the error  
314 associated with the spatial variability of the reference inventory ( $\pm 20 \text{ Bq kg}^{-1}$ )  
315 were propagated through the conversion model in order to receive an upper  
316 and lower confidence interval for the resulting erosion estimates.

#### 317 2.4 Spatial modelling of snow glide distances

318 We used the Spatial Snow Glide Model (SSGM, Leitinger et al. 2008) to predict  
319 potential snow glide distances for an area of approximately  $30 \text{ km}^2$  surrounding  
320 our study sites. The SSGM is an experimental model, which includes the  
321 parameters: the forest stand, the slope angle, the winter precipitation, the slope  
322 and the static friction coefficient  $\mu_s$  (-). Slope angle and slope aspect were  
323 derived from the digital elevation models DHM25 and below 2000 m a.s.l. the  
324 DOM. The DOM is a high precision digital surface model with 2 m resolution and  
325 an accuracy of  $\pm 0.5 \text{ m}$  at  $1\sigma$  in open terrain and  $\pm 1.5 \text{ m}$  at  $1\sigma$  in terrain with  
326 vegetation. The DHM25 has a resolution of 25 m with an average error of 1.5 m  
327 for the Central Plateau and the Jura, 2 m for the Pre-Alps and the Ticino and 3  
328 to 8 m for the Alps (Swisstopo). Winter precipitation was derived from the  
329 MeteoSwiss station located in Andermatt. We used the result from a QuickBird  
330 land cover classification with a resolution of 2.4 m (subsequently resampled to 5  
331 m) as land cover input (Meusbürger et al., 2010a). Combining this land cover  
332 map with a land use map (Meusbürger and Alewell, 2009), it was possible to  
333 derive the parameter forest stand. To each of the 4 investigated land cover  
334 types a uniform static friction coefficient ( $\mu_s$ ) was assigned.

335 The static friction coefficient can be derived by:

$$336 \mu_s = \frac{F_r}{F_n} \quad \text{Equation 6}$$

337 where  $F_n$  ( $\text{g m s}^{-2}$ ) is the normal force that can be calculated with

338  $F_n = m \times g \times \cos \alpha$

Equation 7

339 where  $g$  is the standard gravity (9.81 m s<sup>-2</sup>),  $\alpha$  is the slope angle (°) and  $m$  the  
340 weight of the snow glide shoe (in our study 202 g).

341 The initial force ( $Fr$ ; with the unit g m s<sup>-2</sup>), which is needed to get the glide shoe  
342 moving on the vegetation surface, was measured with a spring balance (Pesola®  
343 Medio 1000 g) and multiplied with the standard gravity. To obtain representative  
344 values of  $Fr$  the measurement was replicated 10 times per sample site and  
345 subsequently averaged. The parameter estimates the surface roughness, which  
346 integrates the effect of different vegetation types and land uses on snow  
347 gliding. A detailed description of the model and its parameters has been  
348 provided by Leitinger et al. (2008).

349 Supplemented by snow glide measurements from this study, the SSGM (i.e. OLS  
350 regression equation) was refined to be valid also for north exposed sites and  
351 sites with *Alnus viridis*. Consequently, the revised SSGM is given by the equation:

352  $\ln(\hat{y}) = -0.337 - 0.925x_1 + 0.095x_2 + 0.01x_3 + 1.006x_4 + 0.839x_5 + 0.076x_6 - 0.075x_7^2$  Equation 8

353 where  $\hat{y}$  is the estimated snow-gliding distance (mm),  $x_1$  is the forest stand (0;1),  
354  $x_2$  is slope angle (°),  $x_3$  is winter precipitation (mm),  $x_4$  is slope aspect East (0;1),  
355  $x_5$  is slope aspect South (0;1),  $x_6$  is slope aspect W (0;1) and  $x_7$  is the static  
356 friction coefficient. The revised SSGM was highly significant ( $p < 0.001$ ) with a  
357 determination coefficient of 0.581 (adjusted R<sup>2</sup>).

358 The model was then applied for the winter period 2009/2010 (285 mm winter  
359 precipitation) and for the long-term average winter precipitation (430 mm  
360 winter precipitation, years 1959 to 2010).

### 361 3 Results and Discussion

#### 362 3.1 Snow glide measurements 2009/2010

363 For each site the static friction coefficient as a measure for surface roughness  
364 was determined in autumn prior to the installation of the snow glide shoes.  
365 Lowest surface roughness was observed for the hayfields, followed by soil  
366 surface at sites covered with *Alnus viridis* on the north facing slope (Table 1). For  
367 the pastures without dwarf-shrubs, the two mean monitored values differed ( $\mu_s =$   
368 0.37 and 0.68) but were similar to that of pastures with dwarf-shrubs ( $\mu_s = 0.66$  to  
369 0.69). Slightly higher values were observed for the dense undergrowth of *Alnus*  
370 *viridis* sites on the south facing slope ( $\mu_s = 0.70$  and 0.84). These static friction  
371 coefficients are within the range of 0.22-1.18 reported by Leitinger et al. (2008).  
372 The snow glide measurements confirmed the presence and the potential impact  
373 of this process in our investigated sites. The mean measured snow glide  
374 distances (sgd) of the different sites varied from 2 to 189 cm (see Table 1). A  
375 main proportion of this variability can be explained by the slope aspect and the  
376 surface roughness (see Fig. 3). With increasing surface roughness (expressed as  
377 the static friction coefficient;  $\mu_s$ ) the snow glide distance declines. This decrease  
378 is more pronounced for the south facing slope (sgd =  $-1547.2\mu_s + 172.93$ ;  $R^2 =$   
379 0.50;  $p = 0.036$ ). For the north facing slope the snow glide distances and the  
380 variability are lower. Approximately 80% of the observed variability on the north  
381 facing slope can be explained by the surface roughness (sgd =  $-622.17\mu_s + 43.09$ ;  
382  $R^2 = 0.82$ ;  $p = 0.033$ ). The identification of slope aspect and surface roughness as  
383 main causal factors for snow gliding, corresponds to the findings of other studies  
384 (In der Gand and Zupancic, 1966; Newesely et al., 2000; Hoeller et al., 2009).  
385 According to several studies on the seasonal snow – soil interface conditions (In  
386 der Gand and Zupancic, 1966; McClung and Clarke, 1987; Leitinger et al., 2008),

387 snow gliding on south-facing sites is preferential in spring, when high solar  
388 radiation leads to a high portion of melting water at the soil/snow interface.  
389 However, in autumn snow gliding primarily occurs when a huge amount of snow  
390 falls on the warm soil. In this case, north-facing sites may be confronted with  
391 high snow gliding activity as well.

392 Our measured snow glide distances are comparable to those recorded by other  
393 researchers. For example Höller et al. (2009) monitored during a seven-year  
394 period in the Austrian Alps a snow glide distance of 10 cm within the forest, 170  
395 cm in cleared forest sites and up to 320 cm for open fields. Margreth (2007)  
396 found total glide distances of 19 to 102 cm for an eleven-year observation  
397 period in the Swiss East Alps (south-east facing slope at 1540 m a.s.l.).

### 398 3.2 Soil erosion estimates

399 Snow glide depositions were observed for seven sites, for one site a wet  
400 avalanche deposition (pN) and for 4 sites no snow glide depositions were  
401 observed (Table 3). The 4 sites without snow glide depositions were all located  
402 at the north facing slope. The erosion rates estimated from the sediment yields  
403 of the snow glide deposition ranged from 0.03 to 22.9 t ha<sup>-1</sup> yr<sup>-1</sup>. The maximum  
404 value was determined for the site h1 which is in agreement with the <sup>137</sup>Cs  
405 method. For sites with snow glide depositions, a mean value of 8.4 t ha<sup>-1</sup> yr<sup>-1</sup> was  
406 measured. The somewhat high erosion rates are documented in a photo from  
407 the spring (Fig. 4). The winter 2012/2013 precipitation of 407 mm was quite  
408 representative of the long-term average (i.e. 430 mm). On average, the  
409 pastured sites without dwarf shrubs produced the highest measured sediment  
410 yields, followed by the hayfields and considerably lower values were observed  
411 for the pastures with dwarf shrub sites. Whether the observed difference is due  
412 to the different vegetation cover or due to site specific topography cannot be



413 solved conclusively with the present dataset. A wet avalanche was observed for  
414 the site pN. Interestingly, the estimated erosion rate of the wet avalanche  
415 deposition was smaller than most of the snow gliding related erosion rates, at  
416  $1.97 \text{ t ha}^{-1} \text{ yr}^{-1}$ . However, high erosion rates of 3.7 and  $20.8 \text{ t ha}^{-1}$  per winter due  
417 to wet avalanches have been reported in a study site located in the Aosta  
418 Valley, Italy (Ceaglio et al., 2012). In this study site where the major soil loss is  
419 triggered by wet avalanches, the snow-related soil erosion estimated from the  
420 deposition area was comparable to the yearly total erosion rates assessed with  
421 the  $^{137}\text{Cs}$  method ( $13.4$  and  $8.8 \text{ t ha}^{-1} \text{ yr}^{-1}$ , Ceaglio et al., 2012).

422 On the north facing slope an average RUSLE estimate of  $1.8 \text{ t ha}^{-1} \text{ yr}^{-1}$  with a  
423 maximum value of  $3.8 \text{ t ha}^{-1} \text{ yr}^{-1}$  was established (Table 2). The on average lower  
424 values as compared to the south-facing slope ( $6.7 \text{ t ha}^{-1} \text{ yr}^{-1}$ ) are due to lower  
425 slope angles (thus lower LS-factor values) and C-factors (due to a higher  
426 fractional vegetation cover). This effect was not compensated by the on  
427 average higher K-factor of  $0.40 \text{ kg h N}^{-1} \text{ m}^{-2}$  on the north facing slopes. The  
428 higher K-factor is caused by a 6 % higher proportion of very fine sand. The mean  
429 RUSLE based soil erosion rate for all sites was  $4.6 \text{ t ha}^{-1} \text{ yr}^{-1}$ .

430 The mean  $^{137}\text{Cs}$  based soil erosion rates of  $17.8 \text{ t ha}^{-1} \text{ yr}^{-1}$  are approximately four  
431 times as high as the average RUSLE estimates. Congruent with RUSLE the  $^{137}\text{Cs}$ -  
432 based average soil erosion rate on the north facing slopes is lower than on the  
433 south facing slopes (by  $8.7 \text{ t ha}^{-1} \text{ yr}^{-1}$ ). The highest  $^{137}\text{Cs}$ -based soil erosion  
434 estimates are found at two hayfield sites (h1 and h3) and the pasture sites at the  
435 south facing slope (p1 and p2). The higher RUSLE and  $^{137}\text{Cs}$  estimates on the  
436 more intensely used, steeper and more snow glide affected south facing slope  
437 are reasonable. However, the high  $^{137}\text{Cs}$ -based erosion rates ( $16.6 \text{ t ha}^{-1} \text{ yr}^{-1}$  for  
438 A1N and  $13.7 \text{ t ha}^{-1} \text{ yr}^{-1}$  for A2N)) at *Alnus viridis* sites are unexpected and will be  
439 discussed below.

440 3.3 *Relation between soil redistribution and snow gliding*

441 Sediment yield measurements in snow glide depositions showed the importance  
442 of this process in the winter 2012/2013. However, even though the winter was  
443 quite representative for the average winter conditions (in terms of winter  
444 precipitation) the measured rates are likely to vary between different years. To  
445 assess the relevance of this process for a longer time scale, a second approach  
446 using RUSLE and  $^{137}\text{Cs}$  was followed.

447 Our hypothesis was that the difference of the water soil erosion rate modelled  
448 with RUSLE and the total net erosion measured with the  $^{137}\text{Cs}$  method correlates  
449 to a "winter soil erosion rate". This winter soil erosion rate comprises long-term  
450 soil removal by snow gliding and occasionally wet avalanches as well as snow  
451 melt. These "winter erosion rates" (difference of  $^{137}\text{Cs}$  and RUSLE) ranged from  
452 rates of  $-7.3 \text{ t ha}^{-1} \text{ yr}^{-1}$  for a pasture with dwarf shrubs to rates of  $31 \text{ t ha}^{-1} \text{ yr}^{-1}$  for  
453 the hayfield site h1. A negative difference of  $^{137}\text{Cs}$  and RUSLE indicates,  
454 according to our hypothesis, a sedimentation (because RUSLE simulates the  
455 potential water soil erosion rates) and a positive value erosion due to processes  
456 not implemented in the RUSLE. The most likely processes would be snow induced  
457 processes. Two observations underpin our hypothesis: first, even though the  
458 sediment yield measurements in the snow glide deposition comprise only one  
459 winter, a relation ( $p = 0.13$ ) between the snow glide erosion and the difference  
460 of  $^{137}\text{Cs}$  and RUSLE could be observed ( $R^2 = 0.39$ ; Fig. 5). The largest difference  
461 between  $^{137}\text{Cs}$  and RUSLE based erosion could be observed for sites with high  
462 snow glide related sediment yield (except for the site h3). The resulting intercept  
463 might be either to a deviation of the weather conditions in the winter 2012/2013  
464 from the long-term average condition captured by the other methods or due to  
465 the impact of occasional wet avalanches and/or snow melt. For instance,

466 following the USLE snow melt adaptation for R-factor would result in an on  
467 average  $2.1 \text{ t ha}^{-1} \text{ yr}^{-1}$  higher modelled erosion rate for all sites.

468 A further indication for the importance of snow gliding as soil erosion agent is  
469 given by the significant positive correlation between measured snow glide  
470 distance and the difference of  $^{137}\text{Cs}$  and RUSLE, which we interpret as winter soil  
471 erosion rate (Fig. 6). The measured snow glide distance explained 64 % of the  
472 variability of the winter soil erosion rate ( $p < 0.005$ ). However, this relation does  
473 not comprise the *Alnus viridis* sites that showed a large difference between  
474 RUSLE and  $^{137}\text{Cs}$  based rates but a low snow glide distance. For the *Alnus viridis*  
475 sites, we have to expect that either one of the two approaches to determine soil  
476 erosion rates is erroneous and/or that we have another predominant erosion  
477 process not considered/or not correctly parameterised in the RUSLE yet. A  
478 possible error related to the  $^{137}\text{Cs}$  approach might be that  $^{137}\text{Cs}$  was intercepted  
479 by leaf and litter material of *Alnus viridis*. Thus, a reference site with *Alnus viridis*  
480 stocking would be necessary which is difficult to find in our site because no flat  
481 areas exist with *Alnus viridis* stocking. The observation of increasing soil erosion  
482 with increasing snow glide rates is congruent with the findings of Leitinger et al.  
483 (2008), who observed that the severity of erosion attributed to snow gliding (e.g.  
484 torn out trees, extensive areas of bare soil due to snow abrasion, landslides in  
485 topsoil) was high in areas with high snow glide distance and vice versa.

486 Generally, for these sub-alpine sites the magnitude of the RUSLE based water  
487 erosion rates need to be considered with caution not only with respect to the  
488 involved uncertainties but also conceptually since several of the factors lay  
489 outside the empirical RUSLE framework. Also the magnitude of the  $^{137}\text{Cs}$  based  
490 erosion rate needs to be considered carefully. The profile distribution model  
491 tends to overestimate soil erosion rates since it assumes that the  $^{137}\text{Cs}$  depth  
492 distribution does not change with time. However, in the very first years after the  
19

493 fallout,  $^{137}\text{Cs}$  was concentrated more in the surface soil layer (Schimmack and  
494 Schultz, 2006). Thus, in the years after the fallout small losses of soil would have  
495 resulted in a relatively high  $^{137}\text{Cs}$  loss which might result in an overestimation of  
496 soil erosion rates.

497 The latter uncertainties do not include snow melt erosion and temporal  
498 variability, both potential reasons for the intercept observed between the  
499 magnitude of winter erosion estimated from RUSLE/ $^{137}\text{Cs}$  and from snow glide  
500 depositions. Nonetheless, the almost 1:1 relation is a clear indication that the  
501 observed discrepancies between the RUSLE and  $^{137}\text{Cs}$  based soil erosion rates  
502 are related to snow gliding. Congruent with our results Stanchi et al. (2014,  
503 accepted) found a relation between the intensity of snow erosion affected  
504 areas and the difference of RUSLE and  $^{137}\text{Cs}$  estimates.

505 Further, it can be deduced that low surface roughness is correlated to high snow  
506 glide distances and these are again positively correlated to large observed  
507 differences between RUSLE and  $^{137}\text{Cs}$  based soil erosion rates that we interpret  
508 as high winter soil erosion rates. Erosion estimates from sediment yield  
509 measurements of the snow glide deposition could confirm the partially high  
510 winter erosion rates. However, the presented relations might be highly variable,  
511 depending on soil temperature (whether the soil is frozen or not) during snow in,  
512 the occurrence of a water film that allows a transition of dry to wet gliding  
513 (Haefeli, 1948) and on the weather conditions of a specific winter. In addition,  
514 some of the investigated sites might also be affected by avalanches in other  
515 years.

### 516 3.4 Modelled snow glide distances

517 The modelled snow glide rates from the SSGM compared reasonably well with  
518 the snow glide measurements (Fig. 7). In agreement with the measured values

519 all sites facing to the north revealed lower modelled snow glide distances.  
520 Largest discrepancies between the mean modelled and measured values of  
521 each site occur for the pastures on the south facing slopes (p and pw). The  
522 model overestimates the snow glide rates for these sites, which might be due to  
523 the effect of micro-relief in form of cattle trails at these sites. This small terraces  
524 (0.5 m in width) most likely reduce snow gliding but are not captured by the  
525 digital elevation model that is used for the SSGM. In general, modelled snow  
526 glide distances show smaller ranges than measured snow glide distances, due to  
527 the 5 m resolution of the model input data (Fig. 7). Interestingly, the occurrence  
528 of dwarf shrubs seems to reduce snow gliding to a larger extend as predicted by  
529 the model.

530 The modelled snow glide distance map (Fig. 8) is based on the long-term  
531 average of winter precipitation, which is with 430 mm clearly higher than the  
532 winter precipitation in 2009/2010 with 285 mm (Fig. 7). The highest snow glide  
533 values were simulated on the steep, south facing slopes with predominate  
534 grassland and dwarf-shrub cover. Very high rates are also found on the lower  
535 parts of the south facing slopes that are used as pastures and hayfields. The  
536 smallest snow glide rates are located on the north facing slopes. The map  
537 clearly reproduces the effect of topography and aspect. Moreover, snow glide  
538 distances summarized for predominant land-use types also reproduce the  
539 impact of vegetation cover (Fig. 9). The highest potential snow glide distances  
540 were simulated by the SSGM for the south-facing hayfield and pasture sites while  
541 the *Alnus viridis* has on average decisively smaller snow glide distances. In  
542 contrast, on the north facing slopes there is no difference observed between  
543 the *Alnus viridis* - and the hayfield category. Here the pasture sites show the  
544 highest average snow glide rate. The interpretation of the differences between

545 land use types is, however, restricted since systematically different topographic  
546 conditions are involved.

547 The topographic and climatic conditions in our valley resemble the environment  
548 under which the SSGM was initially developed; nonetheless further regular yearly  
549 measurement would be needed to improve the performance of the model in this  
550 area. In conclusion, the application of the SSGM highlighted the relevance of  
551 the snow gliding process and the potentially related soil erosion for (sub-) alpine  
552 areas.

#### 553 **4 Conclusions**

554 The presented absolute magnitude of the snow glide related soil erosion rate is  
555 subject to high inter-annual variability. However, snow glide erosion measured  
556 from the snow glide depositions (0.03 to 22.9 t ha<sup>-1</sup> yr<sup>-1</sup> in the winter 2012/2013)  
557 highlights the need to consider the process of snow gliding as a soil erosion  
558 agent in steep, scarcely vegetated alpine areas.

559 RUSLE and <sup>137</sup>Cs both yield average long-term soil erosion rates for water and  
560 total net erosion, respectively. Despite the associated uncertainties, the total  
561 net erosion rate is significantly higher than the gross water erosion rate provided  
562 by RUSLE. We interpret the difference as "winter" soil erosion rate which was  
563 significantly correlated to snow glide rates and showed an almost 1:1 relation to  
564 sediment yield measurements in snow glide depositions. The application of RUSLE  
565 and <sup>137</sup>Cs showed i) the relevance of the snow glide process for a longer time  
566 scale (as compared to the snow glide deposition measurements of one winter)  
567 and ii) that for an accurate soil erosion prediction in high mountain areas it is  
568 crucial to assess and quantify the erosivity of snow movements.

569 The Spatial Snow Glide Model might serve as a tool to evaluate the spatial  
570 relevance of snow gliding for larger areas. However, it would be recommended

571 to additionally estimate the kinetic energy that acts upon the soil during the  
572 snow movement. This would allow for a direct comparison of rainfall erosivity  
573 and snow movement erosivity, and moreover its insertion into soil erosion risk  
574 models. The impact of snow movement on soil removal should moreover, be  
575 evaluated in context of predicted changes in snow cover e.g. an increase of  
576 snow amount for elevated (>2000 m a.s.l.) areas (Beniston, 2006).

577 Further, we demonstrated that surface roughness, which is determined by the  
578 vegetation type and the land use, reduces snow glide rates particularly on the  
579 in general more intensely used south facing slopes. In turn snow glide rates are  
580 positively related to increasing soil loss for grassland sites. This is an important  
581 result with respect to soil conservation strategy since surface roughness can be  
582 modified and adapted through an effective land use management.

583

584 Acknowledgement

585 This study was funded by the Swiss Federal Office for the Environment (Contract-  
586 no.: StoBoBio/810.3129.004/05/0X).

587



588

589

## References

590

591 Ackroyd, P.: Erosion by snow avalanche and implications for geomorphic  
592 stability, Torlesse Range, New-Zealand, *Arct. Alp. Res.*, 19, 65-70,  
593 10.2307/1551001, 1987.

594 Ajayi, I. R., Fischer, H. W., Burak, A., Qwasmeh, A., and Tabot, B.: Concentration  
595 and vertical distribution of Cs-137 in the undisturbed soil of southwestern  
596 Nigeria, *Health Phys.*, 92, 73-77, 2007.

597 Alewell, C., Meusburger, K., Juretzko, G., Mabit, L., and Ketterer, M.: Suitability of  
598 <sup>239+240</sup>Pu as a tracer for soil erosion in alpine grasslands, *Chemosphere*, 103, 274-  
599 280, doi: 10.1016/j.chemosphere.2013.12.016., 2014.

600 Arapis, G. D., and Karandinos, M. G.: Migration of Cs-137 in the soil of sloping  
601 semi-natural ecosystems in Northern Greece, *Journal of Environmental*  
602 *Radioactivity*, 77, 133-142, 10.1016/j.jenvrad.2004.03.004, 2004.

603 Bell, I., Gardner, J., and Descally, F.: An estimate of snow avalanche debris  
604 transport, Kaghan Valley, Himalaya, Pakistan, *Arct. Alp. Res.*, 22, 317-321,  
605 10.2307/1551594, 1990.

606 Beniston, M.: Mountain weather and climate: A general overview and a focus on  
607 climatic change in the Alps, *Hydrobiologica*, 562, 3-16, 2006.

608 Benmansour, M., Mabit, L., Nouria, A., Moussadek, R., Bouksirate, H., Duchemin,  
609 M., and Benkdad, A.: Assessment of soil erosion and deposition rates in a  
610 Moroccan agricultural field using fallout <sup>137</sup>Cs and <sup>210</sup>Pbex, *Journal of*  
611 *Environmental Radioactivity*, 115, 97-106, 10.1016/j.jenvrad.2012.07.013, 2013.

612 Ceaglio, E., Meusburger, K., Freppaz, M., Zanini, E., and Alewell, C.: Estimation of  
613 soil redistribution rates due to snow cover related processes in a mountainous  
614 area (Valle d'Aosta, NW Italy), *Hydrology and Earth System Sciences*, 16, 517-  
615 528, 2012.

616 Confortola, G., Maggioni, M., Freppaz, M., and Bocchiola, D.: Modelling soil  
617 removal from snow avalanches: A case study in the North-Western Italian Alps,  
618 Cold Regions Science and Technology, 70, 43-52,  
619 10.1016/j.coldregions.2011.09.008, 2012.

620 Foster, G. R., and Highfill, R. E.: Effect of terraces on soil loss - USLE P-factor  
621 values for terraces, Journal Of Soil And Water Conservation, 38, 48-51, 1983.

622 Freppaz, M., Godone, D., Filippa, G., Maggioni, M., Lunardi, S., Williams, M. W.,  
623 and Zanini, E.: Soil Erosion Caused by Snow Avalanches: a Case Study in the  
624 Aosta Valley (NW Italy), Arct. Antarct. Alp. Res., 42, 412-421, 10.1657/1938-4246-  
625 42.4.412, 2010.

626 Fuchs, S., and Keiler, M.: Variability of Natural Hazard Risk in the European Alps:  
627 Evidence from Damage Potential Exposed to Snow Avalanches, Disaster  
628 Mangement Handbook, edited by: Pinkowski, J., Crc Press-Taylor & Francis  
629 Group, Boca Raton, 267-279 pp., 2008.

630 Gardner, J. S.: Observations on erosion by wet snow avalanches, Mount Rae  
631 area, Alberta, Canada, Arct. Alp. Res., 15, 271-274, 10.2307/1550929, 1983.

632 Haefeli, R.: Schnee, Lawinen, Firn und Gletscher, Ingenieur-Geologie, edited by:  
633 Bendel, L., Springer Vienna, Wien, 1948.

634 Heckmann, T., Wichmann, V., and Becht, M.: Sediment transport by avalanches  
635 in the Bavarian Alps revisited - a perspective on modelling, in: Geomorphology  
636 in Environmental Application:, edited by: Schmidt, K. H., Becht, M., Brunotte, E.,  
637 Eitel, B., and Schrott, L., Zeitschrift Fur Geomorphologie Supplement Series,  
638 Gebruder Borntraeger, Stuttgart, 11-25, 2005.

639 Hoeller, P., Fromm, R., and Leitinger, G.: Snow forces on forest plants due to  
640 creep and glide, Forest Ecology and Management, 257, 546-552,  
641 10.1016/j.foreco.2008.09.035, 2009.

642 Holler, P., Fromm, R., and Leitinger, G.: Snow forces on forest plants due to  
643 creep and glide, Forest Ecology and Management, 257, 546-552,  
644 10.1016/j.foreco.2008.09.035, 2009.

645 In der Gand, H. R., and Zupancic, M.: Snow gliding and avalanches, IAHS-AISH  
646 Publ, 69, 230-242, 1966.

647 Jomelli, V., and Bertran, P.: Wet snow avalanche deposits in the French Alps:  
648 Structure and sedimentology, *Geogr. Ann. Ser. A-Phys. Geogr.*, 83A, 15-28,  
649 10.1111/j.0435-3676.2001.00141.x, 2001.

650 Juretzko, G.: Quantifizierung der Bodenerosion mit <sup>137</sup>Cs und USLE in einem  
651 alpinen Hochtal (Val Piora, CH), Master, Environmental Sciences, Basel, Basel, 1-  
652 152 pp., 2010.

653 Kinnell, P. I. A.: Why the universal soil loss equation and the revised version of it  
654 do not predict event erosion well, *Hydrological Processes*, 19, 851-854,  
655 10.1002/hyp.5816, 2005.

656 Kinnell, P. I. A.: Event soil loss, runoff and the Universal Soil Loss Equation family  
657 of models: A review, *Journal of Hydrology*, 385, 384-397,  
658 10.1016/j.jhydrol.2010.01.024, 2010.

659 Kirchner, G.: Establishing reference inventories of Cs-137 for soil erosion studies:  
660 Methodological aspects, *Geoderma*, 211, 107-115,  
661 10.1016/j.geoderma.2013.07.011, 2013.

662 Konz, N., Schaub, M., Prasuhn, V., Bänninger, D., and Alewell, C.: Cesium-137-  
663 based erosion-rate determination of a steep mountainous region, *Journal of*  
664 *Plant Nutrition and Soil Science*, 172, 615-622, 10.1002/jpln.200800297, 2009.

665 Konz, N., Baenninger, D., Konz, M., Nearing, M., and Alewell, C.: Process  
666 identification of soil erosion in steep mountain regions, *Hydrology and Earth*  
667 *System Sciences*, 14, 675-686, 2010.

668 Konz, N., Prasuhn, V., and Alewell, C.: On the measurement of alpine soil  
669 erosion, *CATENA*, 91, 63-71, 10.1016/j.catena.2011.09.010, 2012.

670 Leitinger, G., Holler, P., Tasser, E., Walde, J., and Tappeiner, U.: Development  
671 and validation of a spatial snow-glide model, *Ecological modelling*, 211, 363-  
672 374, 10.1016/j.ecolmodel.2007.09.015, 2008.

673 Mabit, L., Bernard, C., Laverdiere, M. R., Wicherek, S., Garnier, J., and Mouchel,  
674 J. M.: Assessment of soil erosion in a small agricultural basin of the St. Lawrence  
675 River watershed, *Hydrobiologia*, 410, 263-268, 1999.

676 Mabit, L., Bernard, C., and Laverdiere, M. R.: Quantification of soil redistribution  
677 and sediment budget in a Canadian watershed from fallout caesium-137 (Cs-  
678 137) data, *Canadian Journal of Soil Science*, 82, 423-431, 2002.

679 Mabit, L., and Bernard, C.: Assessment of spatial distribution of fallout  
680 radionuclides through geostatistics concept, *Journal of Environmental*  
681 *Radioactivity*, 97, 206-219, 10.1016/j.jenvrad.2007.05.008, 2007.

682 Mabit, L., Benmansour, M., and Walling, D. E.: Comparative advantages and  
683 limitations of the fallout radionuclides Cs-137, Pb-210(ex) and Be-7 for assessing  
684 soil erosion and sedimentation, *Journal of Environmental Radioactivity*, 99, 1799-  
685 1807, 10.1016/j.jenvrad.2008.08.009, 2008.

686 Mabit, L., Meusburger, K., Fulajtar, E., and Alewell, C.: The usefulness of <sup>137</sup>Cs as  
687 a tracer for soil erosion assessment: A critical reply to Parsons and Foster (2011),  
688 *Earth-Science Reviews*, 137, 300-307,  
689 <http://dx.doi.org/10.1016/j.earscirev.2013.05.008>, 2013.

690 Margreth, S.: Snow pressure on cableway masts: Analysis of damages and design  
691 approach, *Cold Regions Science and Technology*, 47, 4-15,  
692 10.1016/j.coldregions.2006.08.020, 2007.

693 Matisoff, G., and Whiting, P. J.: Measuring Soil Erosion Rates Using Natural (Be-7,  
694 Pb-210) and Anthropogenic (Cs-137, Pu-239, Pu-240) Radionuclides, *Handbook of*  
695 *Environmental Isotope Geochemistry*, Vols 1 and 2, edited by: Baskaran, M.,  
696 Springer-Verlag Berlin, Berlin, 487-519 pp., 2011.

697 McClung, D. M., and Clarke, G. K. C.: The effects of free-water on snow gliding,  
698 *Journal of Geophysical Research-Solid Earth and Planets*, 92, 6301-6309, 1987.

699 Merritt, W. S., Letcher, R. A., and Jakeman, A. J.: A review of erosion and  
700 sediment transport models, *Environmental Modelling & Software*, 18, 761-799,  
701 2003.

702 Meusburger, K., and Alewell, C.: On the influence of temporal change on the  
703 validity of landslide susceptibility maps, *Nat Hazard Earth Sys*, 9, 1495-1507, 2009.

704 Meusburger, K., Banninger, D., and Alewell, C.: Estimating vegetation parameter  
705 for soil erosion assessment in an alpine catchment by means of QuickBird  
706 imagery, *International Journal of Applied Earth Observation and*  
707 *Geoinformation*, 12, 201-207, 10.1016/j.jag.2010.02.009, 2010a.

708 Meusburger, K., Konz, N., Schaub, M., and Alewell, C.: Soil erosion modelled with  
709 USLE and PESERA using QuickBird derived vegetation parameters in an alpine  
710 catchment, *International Journal of Applied Earth Observation and*  
711 *Geoinformation*, 12, 208-215, 10.1016/j.jag.2010.02.004, 2010b.

712 Meusburger, K., Mabit, L., Park, J. H., Sandor, T., and Alewell, C.: Combined use  
713 of stable isotopes and fallout radionuclides as soil erosion indicators in a  
714 forested mountain site, South Korea, *Biogeosciences Discuss.*, 10, 2565-2589,  
715 doi:10.5194/bgd-10-2565-2013, 2013.

716 Nearing, M., Foster, G., Lane, L., and Finkner, S.: A process-based soil erosion  
717 model for USDA - water erosion prediction project technology, *Transactions of*  
718 *the American Society of Agricultural Engineers*, 32, 1587-1593, 1989.

719 Newesely, C., Tasser, E., Spadinger, P., and Cernusca, A.: Effects of land-use  
720 changes on snow gliding processes in alpine ecosystems, *Basic and Applied*  
721 *Ecology*, 1, 61-67, 10.1078/1439-1791-00009, 2000.

722 Panagos, P., Meusburger, K., Van Liedekerke, M., Alewell, C., Hiederer, R., and  
723 Montanarella, L.: Assessing soil erosion in Europe based on data collected  
724 through a European Network, *Soil Science and Plant Nutrition*, 1-15,  
725 <http://dx.doi.org/10.1080/00380768.2013.835701>, 2014.

726 Parker, S. P.: McGraw-Hill Dictionary of Scientific and Technical Terms, published  
727 by The McGraw-Hill Companies, Inc., New York City, 2002.

728 Renard, K. G., Foster, G. R., Weesies, G. A., MCCool, D. K., and Yoder, D. C.:  
729 Predicting soil erosion by water; a guide to conservation planning with the  
730 revised universal soil loss equation (RUSLE), US Department of Agriculture, 404,  
731 1997.

732 Riesen, T., Zimmermann, S., and Blaser, P.: Spatial Distribution of <sup>137</sup>Cs in Forest  
733 SOils of Switzerland, *Water, Air, & Soil Pollution*, 114, 277-285,  
734 10.1023/a:1005045905690, 1999.

735 Risse, L. M., Nearing, M. A., Nicks, A. D., and Laflen, J. M.: Error assessment in the  
736 Universal Soil Loss Equation, *Soil Science Society of America Journal*, 57, 825-833,  
737 1993.

738 Rogler, H., and Schwertmann, U.: Rainfall erosivity and isoerodent map of  
739 Bavaria, *Zeitschrift für Kulturtechnik und Flurbereinigung*, 22, 99-112, 1981.

740 Schaub, M., Konz, N., Meusburger, K., and Alewell, C.: Application of in-situ  
741 measurement to determine <sup>137</sup>Cs in the Swiss Alps, *Journal of Environmental*  
742 *Radioactivity*, 101, 369-376, 2010.

743 Schimmack, W., Bunzl, K., and Zelles, L.: Initial rates of migration of radionuclides  
744 from the Chernobyl fallout in undisturbed soils, *Geoderma*, 44, 211-218, 1989.

745 Schimmack, W., and Schultz, W.: Migration of fallout radiocaesium in a grassland  
746 soil from 1986 to 2001 - Part 1: Activity-depth profiles of Cs-134 and Cs-137,  
747 *Science of the Total Environment*, 368, 853-862, 2006.

748 Schuller, P., Bunzl, K., Voigt, G., Ellies, A., and Castillo, A.: Global fallout Cs-137  
749 accumulation and vertical migration in selected soils from South Patagonia,  
750 *Journal of Environmental Radioactivity*, 71, 43-60, 10.1016/s0265-931x(03)00140-1,  
751 2004.

752 Schüpp, M.: Objective weather forecasts using statistical aids in Alps, *Rivista*  
753 *Italiana Di Geofisica E Scienze Affini*, 1, 32-36, 1975.

754 Smith, S. J., Williams, J. R., Menzel, R. G., and Coleman, G. A.: Prediction of  
755 sediment yield from Southern Plains grasslands with the Modified Universal Soil  
756 Loss Equation, *J. Range Manage.*, 37, 295-297, 10.2307/3898697, 1984.

757 Stanchi, S., Freppaz, M., Ceaglio, E., Maggioni, M., Meusburger, K., Alewell, C.,  
758 and Zanini, E.: Soil erosion in an avalanche release site (Valle d'Aosta: Italy):  
759 towards a winter factor for RUSLE in the Alps, *NHESSD*, 2, 1405-1431,  
760 doi:10.5194/nhessd-2-1405-2014, 2014, accepted.

761 Sutherland, R. A.: Caesium-137 soil sampling and inventory variability in  
762 reference locations: A literature survey, *Hydrological Processes*, 10, 43-53, 1996.

763 US Department of Agriculture, S. C. S.: Procedure for computing sheet and rill  
764 erosion on project areas, Soil Conservation Service, Technical Release No. 51  
765 (Rev. 2), 1977.

766 Walling, D. E., Zhang, Y., and He, Q.: Models for deriving estimates of erosion  
767 and deposition rates from fallout radionuclide (caesium-137, excess lead-210,  
768 and beryllium-7) measurements and the development of user friendly software  
769 for model implementation, in: *Impact of Soil Conservation Measures on Erosion  
770 Control and Soil Quality*, 11–33, 2011.

771 Wischmeier, W. H., and Smith, D. D.: Predicting rainfall-erosion losses from  
772 cropland east of the Rocky Mountains, *Agriculture Handbook 282*, US  
773 Department of Agriculture, Washington DC, 1965.

774 Wischmeier, W. H., and Smith, D. D.: Predicting Rainfall Erosion Losses - A Guide  
775 to Conservation Planning, USDA/Science and Education Administration, US.  
776 Govt. Printing Office, Washington D.C., 58 pp., 1978.

777

778

779

780 **5 Tables**

781 Table 1: Parameters related to measured snow glide distance (sgd, SD =  
 782 standard deviation based on 3-5 replicate measurements) for the investigation  
 783 sites in the Ursern Valley, Switzerland. N indicates the sites on the north facing  
 784 slope.

site	vegetation	slope (°)	initial force Fr (g m s <sup>-2</sup> )	static friction coefficient $\mu_s$ (-)	measured sgd (cm)	SD sgd (cm)
h1	hayfield	39	569	0.37	189	117
h2	hayfield	38	510	0.33	50	40
h3	hayfield	35	392	0.24	126	49
pw1	pasture with dwarf- shrubs	38	1030	0.66	34	19
pw2	pasture with dwarf- shrubs	35	1118	0.69	28	15
p1	pasture	38	579	0.37	89	37
p2	pasture	35	1109	0.68	64	40
h1N	hayfield	28	343	0.20	30	14
h2N	hayfield	30	608	0.35	8	1
pN	pasture	18	628	0.33	17	23
A1N	<i>Alnus viridis</i>	25	1050	0.58	2	1
A2N	<i>Alnus viridis</i>	30	451	0.26	28	9
A1	<i>Alnus viridis</i>	22	1550	0.84	14	18
A2	<i>Alnus viridis</i>	31	1197	0.70	60	46

785

786



787

788 Table 2: Measured site characteristics (SOC=soil organic carbon; vfs= very fine sand fraction), resulting RUSLE factors  
 789 and soil erosion rates and <sup>137</sup>Cs based erosion rates for the investigation sites in the Ursern Valley, Switzerland.  
 790 \*indicated the sites from Konz et al. (2009).

site	slope (°)	SOC (%)	vfs (%)	silt (%)	clay (%)	K-factor (kg h N <sup>-1</sup> m <sup>-2</sup> )	P-factor (-)	LS- factor (-)	R- factor (N h <sup>-1</sup> )	C- factor (- )	RUSLE (t ha <sup>-1</sup> yr <sup>-1</sup> )	<sup>137</sup> Cs (t ha <sup>-1</sup> yr <sup>-1</sup> )
h1	39	7.7	12.9	47.3	12.5	0.280	1.00	22.2	97.2	0.010	6.0	37.0
h2	38	7.2	9.7	58.8	17.3	0.290	1.00	8.8	94.5	0.006	1.5	11.0
h3	35	7.4	12.3	43.8	16.9	0.230	1.00	20.7	93.6	0.010	4.5	33.0
pw1	38	6.9	6.3	63.5	10.8	0.320	0.90	12.6	91.7	0.040	13.3	6.0
pw2	35	7.1	11.2	40.9	14.2	0.230	0.90	11.8	94.8	0.040	9.3	13.0
p1	38	7.6	11.2	50.5	11.6	0.270	0.90	11.8	97.6	0.020	5.6	20.0
p2	35	7.2	12.4	45.6	15.0	0.250	0.90	15.3	96.4	0.020	6.6	30.0
h1N	28	4.8	18.5	41.0	5.8	0.416	1.00	7.0	93.6	0.012	3.2	18.3
h2N	30	4.3	13.7	48.0	8.5	0.419	1.00	8.4	91.7	0.012	3.8	7.5
pN	18	6.2	17.5	38.7	10.2	0.369	1.00	1.1	97.2	0.012	0.5	7.2
A1N	25	3.8	16.1	43.8	9.7	0.399	1.00	5.3	93.6	0.003	0.6	16.6
A2N	30	6.8	18.7	39.7	9.6	0.389	1.00	8.4	91.7	0.003	0.9	13.7
Mean of N-facing sites	37	7.3	10.9	50.1	14.0	0.267	0.94	14.7	95.1	0.021	6.7	21.4
Mean of S- facing sites	26	5.2	16.9	42.2	8.8	0.398	1.00	6.0	93.6	0.008	1.8	12.7
mean of all sites	32.4	6.4	13.4	46.8	11.8	0.3	1.0	11.1	94.5	0.0	4.6	17.8

791

792

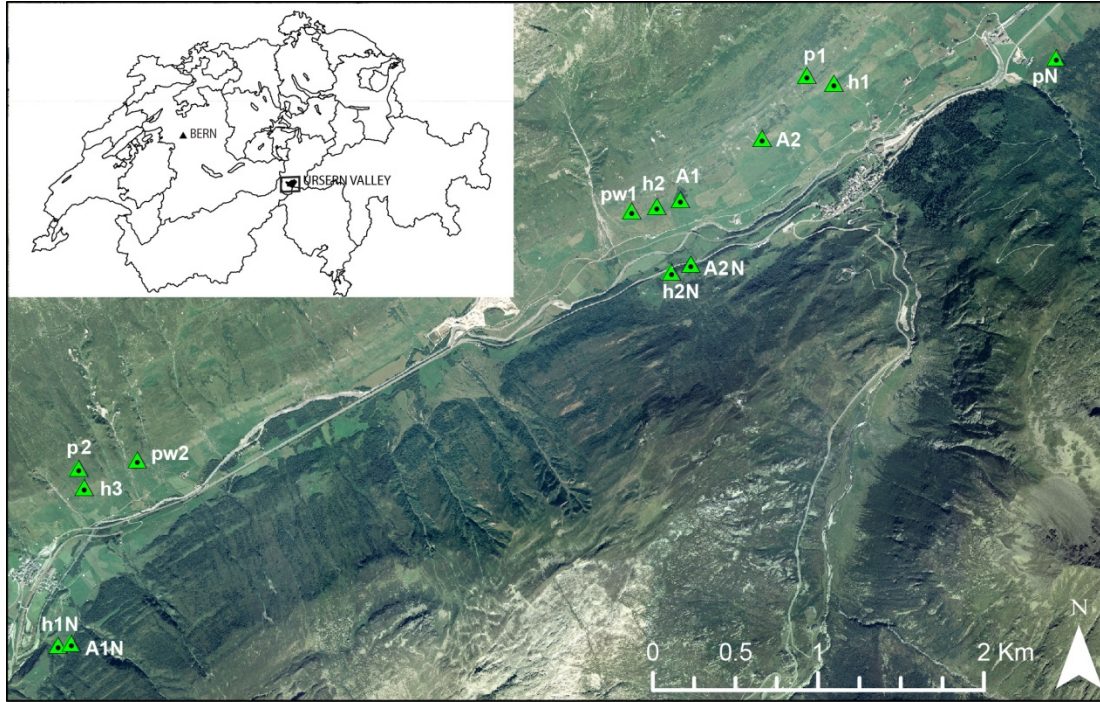
793

794 Table 3: Snow movement related soil erosion derived from the difference of  $^{137}\text{Cs}$ -based and RUSLE-based erosion  
 795 rates (Diff.) and from field measured sediment in snow glide deposits (sg erosion). For each snow glide deposit, the  
 796 mean sediment yield estimate is based on several samples (n). SD = is the standard deviation for the resulting  
 797 erosion rates based on the individual sediment yield samples and \* indicates the sediment yield of a wet avalanche.  
 798 Uncertainty Diff. provides the uncertainty of Diff. resulting from both the  $^{137}\text{Cs}$  and RUSLE method.

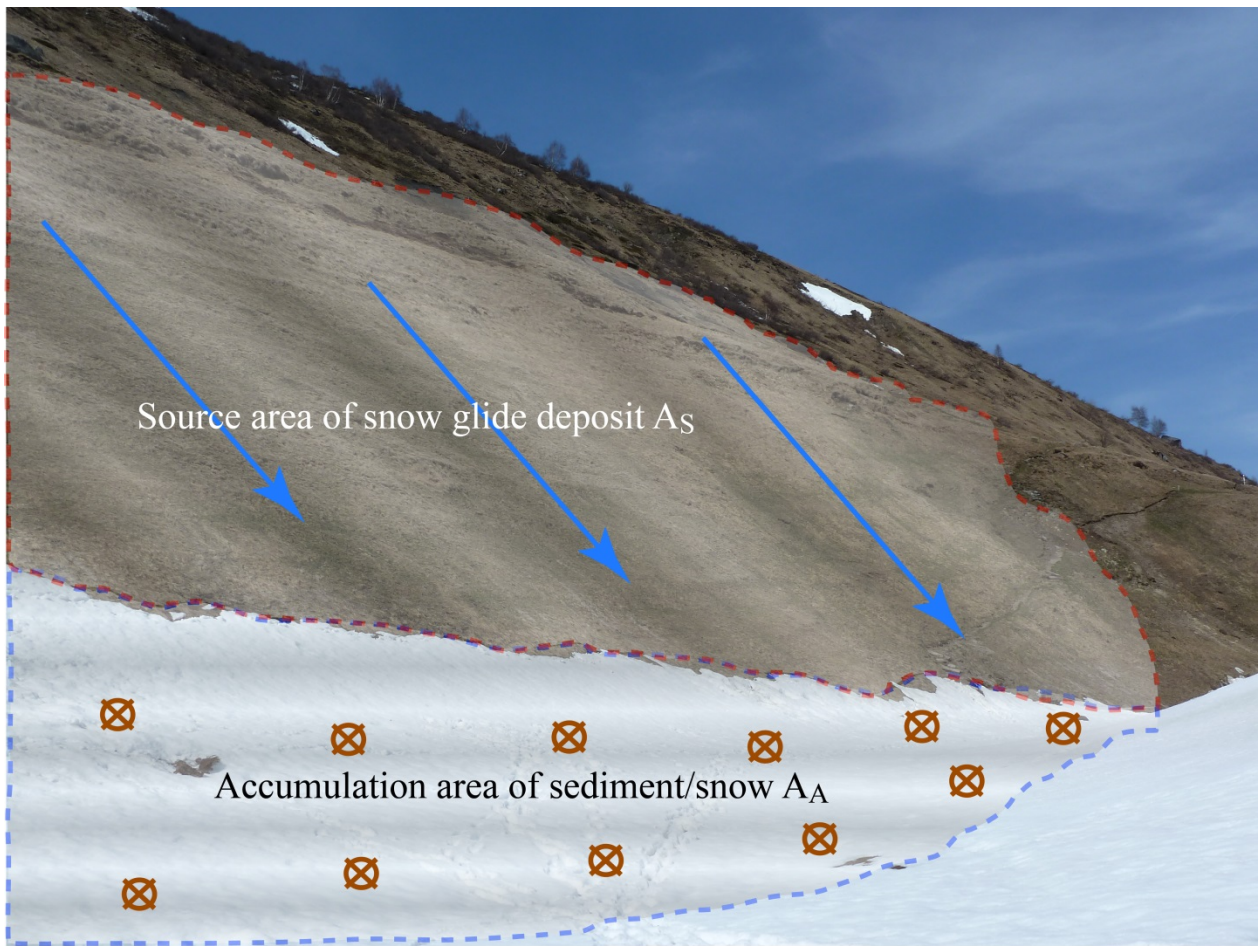
site	RUSLE (t ha <sup>-1</sup> yr <sup>-1</sup> )	$^{137}\text{Cs}$ (t ha <sup>-1</sup> yr <sup>-1</sup> )	Diff. $^{137}\text{Cs}$ - RUSLE (t ha <sup>-1</sup> yr <sup>-1</sup> )	Uncertainty Diff. (t ha <sup>-1</sup> yr <sup>-1</sup> )	sg erosion (t ha <sup>-1</sup> yr <sup>-1</sup> )	SD sg erosion (t ha <sup>-1</sup> yr <sup>-1</sup> )	n
h1	6.0	37.0	31.0	8.5	22.9	81.5	16
h2	1.5	11.0	9.5	7.7	3.2	1.9	3
h3	4.5	33.0	28.5	8.2	1.1	1.9	10
pw1	13.3	6.0	-7.3	10.9	0.8	0.5	3
pw2	9.3	13.0	3.7	9.8	0.0	0.1	7
p1	5.6	20.0	14.4	8.5	16.7	6.8	11
p2	6.6	30.0	23.4	8.6	14.0	44.9	13
h1N	3.2	18.3	15.1	7.6	no snow glide	-	-
h2N	3.8	7.5	3.7	8.4	no snow glide	-	-
pN	0.5	7.2	6.7	8.0	1.97*	3.8	18
A1N	0.6	16.6	16.0	7.2	no snow glide	-	-
A2N	0.9	13.7	12.8	7.6	no snow glide	-	-


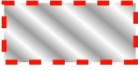


799  
800

801 6 Figure captions



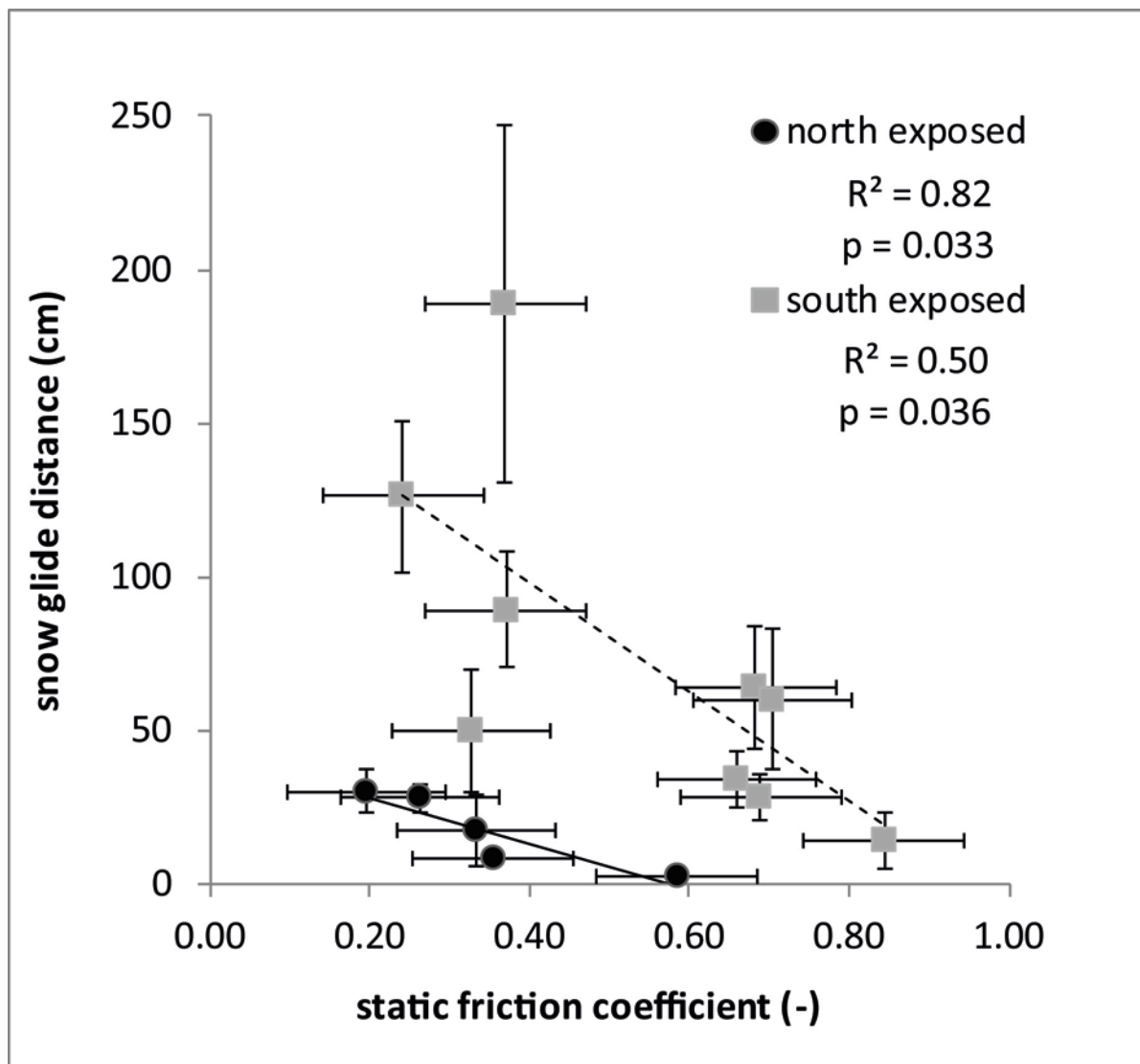
802  
803 Fig. 1 The Ursern Valley in the Central Swiss Alps and the location of the 14  
804 investigated sites (hayfields (h), pastures (p), pastures with dwarf shrubs (pw),  
805 and abandoned grassland covered with *Alnus viridis* (A), north facing slope (N)).



-  Area sampling device  $A_c$
-  Source area of snow glide deposit  $A_S$
-  Accumulation area of sediment/snow  $A_A$
-  Direction of snow gliding

806

807 Fig.2 Illustration of the procedure for snow glide related erosion rate assessment.

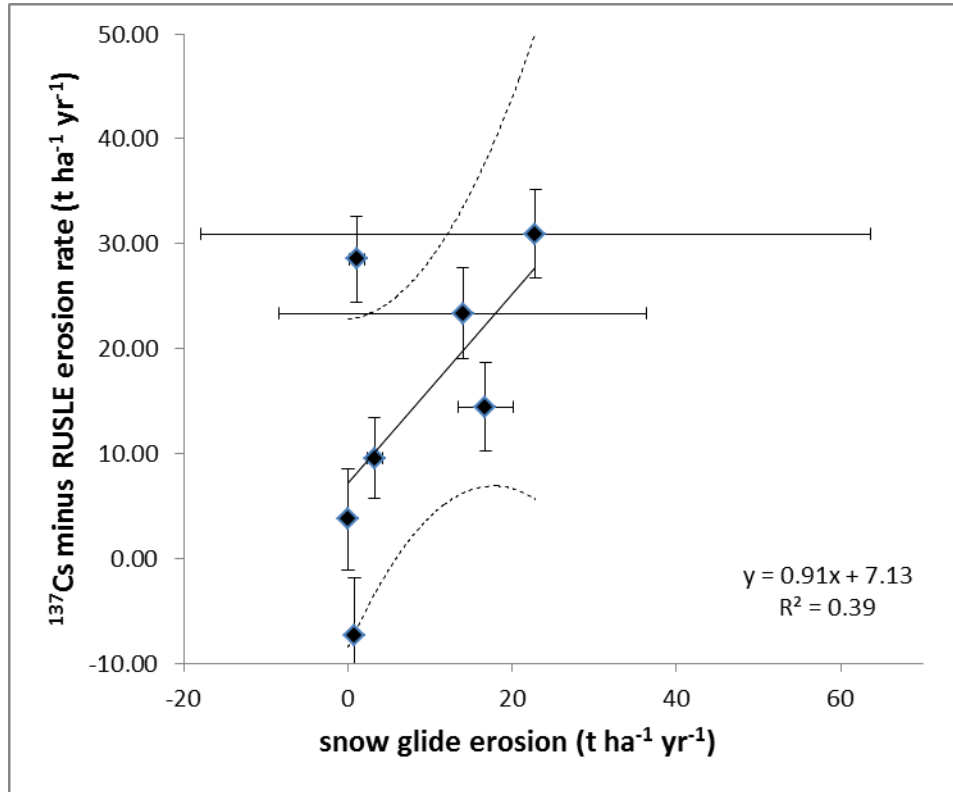


808  
 809 Fig. 3 Snow glide distance against the static friction coefficient for the south-  
 810 (squares) and north (dots) facing slope sites. Y-error bars represent the standard  
 811 deviation of replicate measurements at one site. For the static friction  
 812 coefficient, an error of  $\pm 0.1$  (corresponding to the scale accuracy of the spring  
 813 balance) was assumed.



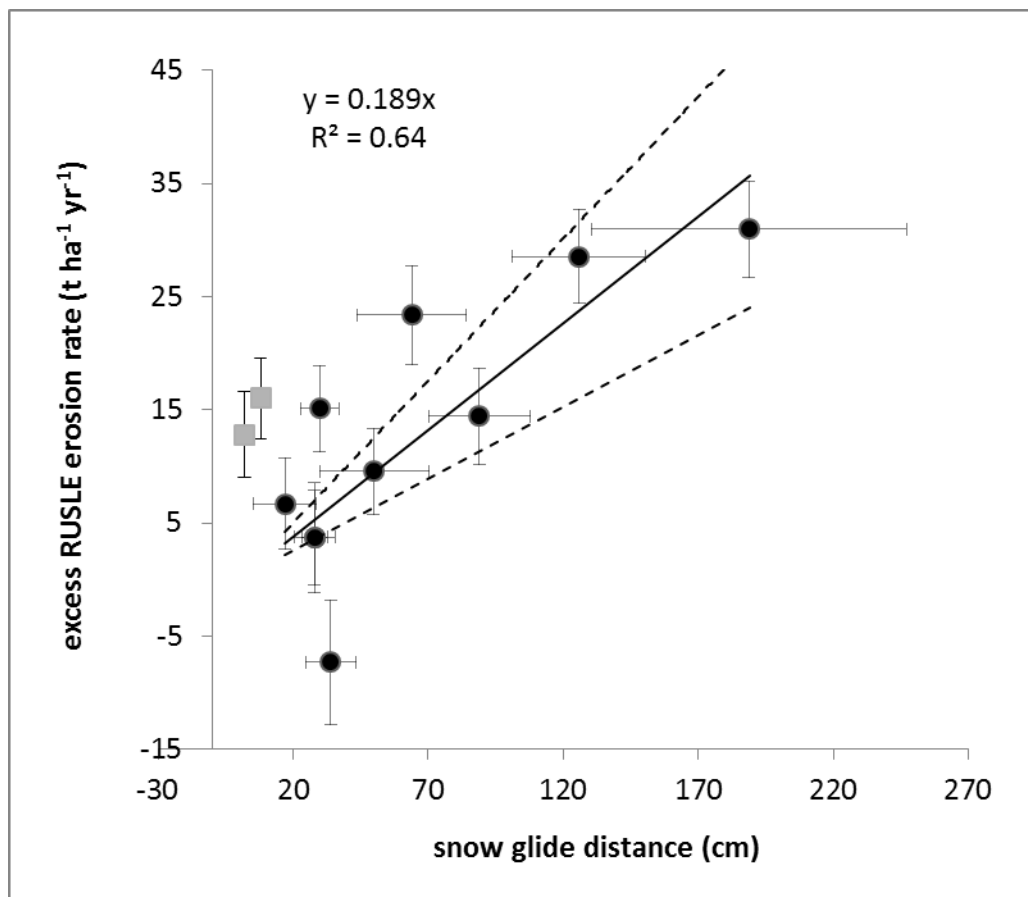
814

815 Fig. 4 Example of snow glide deposits for the site p1.



816

817 Fig. 5 Snow glide erosion estimated from the snow glide deposit sediment yield  
818 against the difference of the <sup>137</sup>Cs and RUSLE soil erosion rate (t ha<sup>-1</sup> yr<sup>-1</sup>). Y-error  
819 bars represent the uncertainty of both the <sup>137</sup>Cs and RUSLE estimates. X-error  
820 bars represent the standard deviation of erosion rates resulting from several  
821 sediment measurements within one snow glide deposit. The solid line represents  
822 the obtained linear regression and the dotted lines the 95% confidence interval.

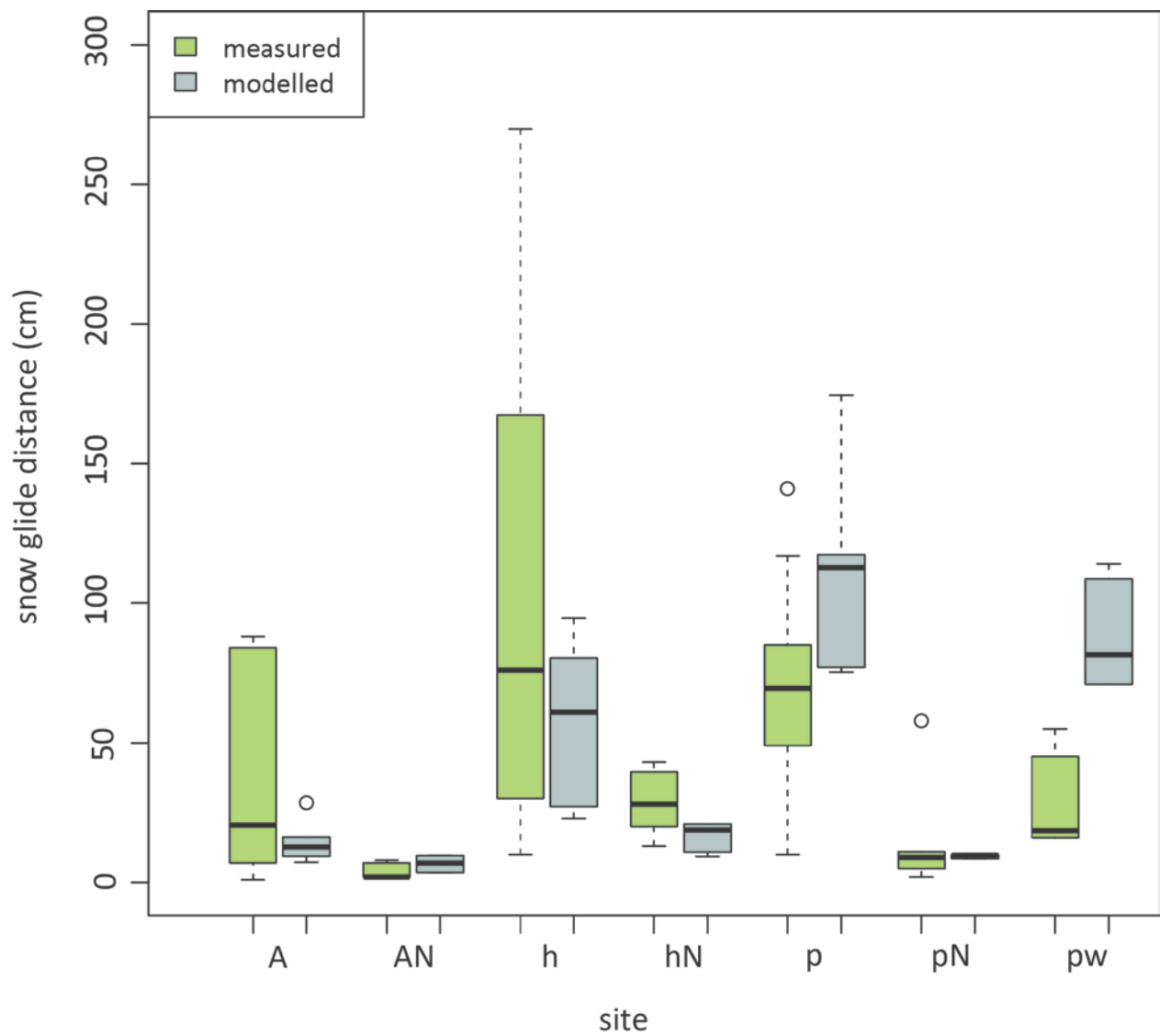


823  
 824 Fig. 6 Correlation of the cumulative snow glide distances (cm) measured for the  
 825 winter 2009/2010 versus the difference of the <sup>137</sup>Cs and RUSLE soil erosion rate (t  
 826 ha<sup>-1</sup> yr<sup>-1</sup>) for the grassland sites (dots, n=10) and the *Alnus viridis* sites A1N, A2N  
 827 (squares, n=2). Y-error bars represent the error of both the <sup>137</sup>Cs and RUSLE  
 828 estimates. X-error bars represent the standard deviation of replicate snow glide  
 829 measurements at one site. Solid line represents a linear regression and the  
 830 dotted lines the 95% confidence interval.

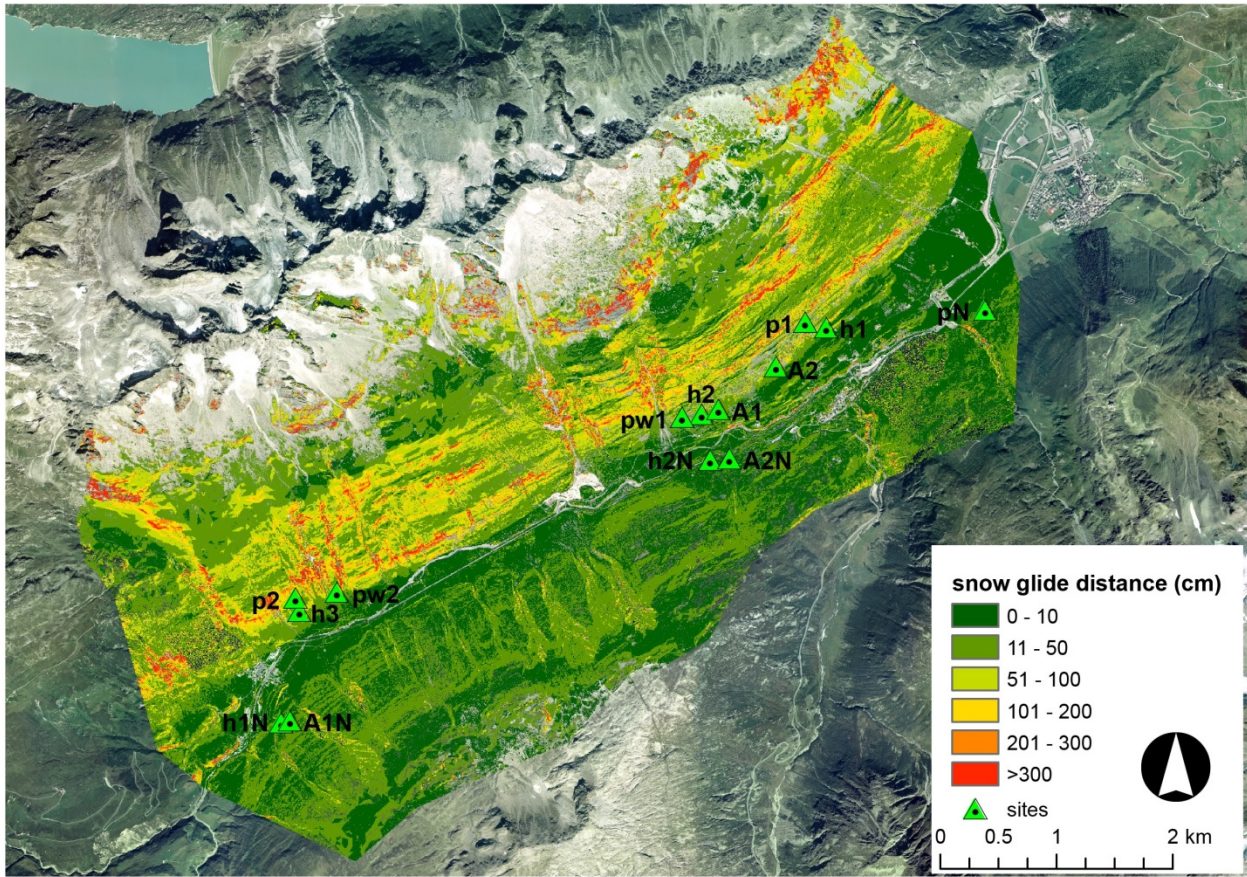
831

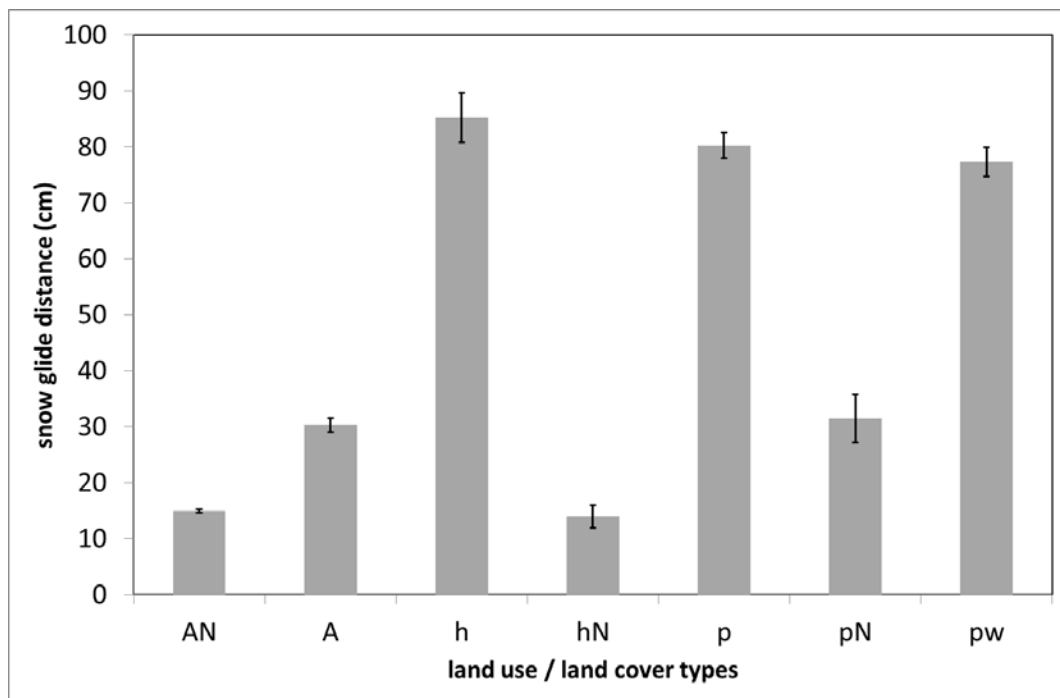
832





833  
 834 Fig. 7 Boxplot of measured snow glide distances and corresponding modelling  
 835 results for different land use/cover types (hayfields (h), pastures (p), pastures  
 836 with dwarf shrubs (pw), and abandoned grassland covered with *Alnus viridis* (A))  
 837 for the winter period 2009/2010. N indicates the sites on the north facing slope.





841  
 842 Fig. 9 Modelled potential snow glide distances (using long-term average winter  
 843 precipitation)) as mean for the whole catchment grouped by predominant land-  
 844 use/cover types (hayfields (h), pastures (p), pastures with dwarf shrubs (pw),  
 845 *Alnus viridis* sites (A)). N indicates the sites on the north facing slope. Error bars  
 846 indicate the standard error of the mean.

847